Journal of Solid State Chemistry **147,** 19–25 (1999)
Article ID jssc.1999.8274, available online at http://www.idealibrary.com on IDEAL®

Giant Negative Magnetoresistance in GdI_2: Prediction and Realization

C. Felser,* K. Ahn,† R. K. Kremer,† R. Seshadri,* and A. Simon†

*Institut für Anorganische Chemie und Analytische Chemie, Johannes Gutenberg Universität, Mainz, Becher Weg 24, 55099 Mainz, Germany; and †Max-Planck-Institut für Festkörperforschung, Heisenbergstraße 1, 70569, Stuttgart, Germany

Received November 5, 1998; in revised form March 9, 1999; accepted March 13, 1999

IN MEMORY OF PROFESSOR JEAN ROUXEL

The electronic structure of the layered d^1 compound GdI_2 has been examined systematically in view of its relation to other layered d^1 systems including superconducting and isostructural $2H$-TaS_2 and $2H$-$NbSe_2$. A van Hove type instability is evident in suitable representations of the Fermi surface. The presence of the half-filled and magnetic $4f$ level should preclude the possibility of superconductivity. Instead GdI_2 orders ferromagnetically at 290(5) K and displays large negative magnetoresistance $\approx$70% at 7 T close to room temperature. This finding provides support to the idea that materials can be searched rationally for interesting properties through high level electronic structure calculations.

I. INTRODUCTION

Achieving specific properties in inorganic materials by design remains a continuing challenge, and revolutionary breakthroughs to this end often seem distant. The more realistic goal of screening existing materials for interesting properties such as superconductivity or magnetoresistance in a rational manner has received a great deal of recent attention. Perhaps the most obvious way of going about this goal is through the careful examination of the crystal and electronic structures of materials known to exhibit these properties. As far as superconductivity is concerned, it has been known for some time that the electronic structures of these compounds show certain patterns of electronic instabilities near the Fermi energy. This is, the flat band–steep band scenario, in particular the van Hove singularity scenario, first proposed to rationalize within the BCS theory, the high transition temperatures of certain intermetallic compounds (1) and later extended to the high temperature cuprate superconductors, approached from the metallic limit (2, 3). In the high temperature superconductors, these instabilities manifest as a specific kind of nesting in the Fermi surface with a characteristic X shape. Through high level electronic structure calculations, known compounds can be screened for this nesting motif suggesting a method for the search for new superconductors.

Through an analysis of the electronic structures of related materials, including $La_2CaCu_2O_6$ (which displays superconductivity) and $LaSr_2Mn_2O_7$ (which displays giant negative magnetoresistance, GMR), it has been shown that despite these compounds showing very different properties, the electronic band structures and the instabilities therein are very similar, the different properties arising through the spin polarization in the case of the manganese oxide (4). The van Hove singularity also seems to be implicated in the mixed-valence behavior of certain europium compounds (5).

Giant negative magnetoresistance is a property that gained recent attention when it was realized in multilayer films of metals (6) and then shown to exist in some perovskite manganates (7, 8) and is associated with a significant decrease in the electrical resistance on applying a magnetic field. In the perovskite manganates, the effects are sufficiently large that the phenomenon has been termed "colossal." Recently, Majumdar and Littlewood (9) have pointed out that for a large class of compounds displaying negative magnetoresistance, there exist certain universal features in the dependence of the magnetoresistance (scaled suitably by the magnetization) on the density of the charge carriers. The perovskite manganates stand out as a unique class of materials since, for a given carrier density, a large range of values of the magnetoresistance is observed. This singular behavior has been ascribed to extensive coupling of the charge, spin, and lattice degrees of freedom in these materials. This is an aspect that we will return to in the discussion.

In a systematic search for magnetic analogues (from the electronic structure viewpoint) of superconductors, our studies have led us to examine GdI_2 (10), a layered d^1 compound that is isostructural (11) with and nominally isoelectronic to the superconductors $2H$-TaS_2 and $2H$-$NbSe_2$. GdI_2 is known to undergo a transition to ferromagnetism close to room temperature (12). Despite the band structure being spin-polarized, as we shall demonstrate, the nature of the conduction band including the nesting motifs

0022-4596/99 $30.00

in suitable visualizations of the Fermi surface show that GdI_2 is indeed closely related to the superconductors. However, the presence of the half-filled $4f$ band results in the compound displaying ferromagnetism. Through use of the systematics seen in the layered manganates and cuprates, we have searched for and indeed found giant negative magnetoresistance with a significant magnitude, approximately 70% at 7 T close to room temperature. Here we present the results, including the electronic structural reasons for the prediction and the experimental realization.

II. COMPUTATIONAL AND EXPERIMENTAL DETAILS

A. Computational Details

GdI_2 crystallizes with the structure of $2H$-MoS_2, comprising infinite GdI_2 sheets with the Gd in the centers of I_6 trigonal prisms (11). Each Gd atom is surrounded by six other Gd atoms in the plane at a distance of 407 pm. The structure of GdI_2 is displayed in Fig. 1. Self-consistent, first principles calculations within the local spin density approximation (LSDA) (13) of the electronic structure of GdI_2 were performed using the LMTO method in the atomic sphere approximation (ASA). A detailed description of the LMTO-ASA method and its application to the electronic band structure of compounds has been given elsewhere (14, 15). The scalar relativistic Kohn–Sham–Schrödinger equations were solved taking all relativistic effects into account except for the spin–orbit coupling. k-space integrations used the tetrahedron method to generate 148 irreducible k-points within the Brillouin zone (BZ). The BZ is as described in Ref. (16), where the special symmetry points are labeled in accordance with the standard notation corresponding to Γ $(0,0,0)$, K $(2/3,1/3,0)$, M $(1/2,0,0)$, A $(0,0,1/2)$, L $(1/2,0,1/2)$, and H $(2/3,1/3,1/2)$ in units of $(2\pi/a, 2\pi/a, 2\pi/c)$. The band structure is displayed along the lines A–Γ, Γ–M, M–K, K–Γ. The basis set consisted of s, d, and f orbitals for Gd and p orbitals for I. The positions and radii of the empty spheres were calculated using an automatic procedure developed by Krier *et al.* (17).

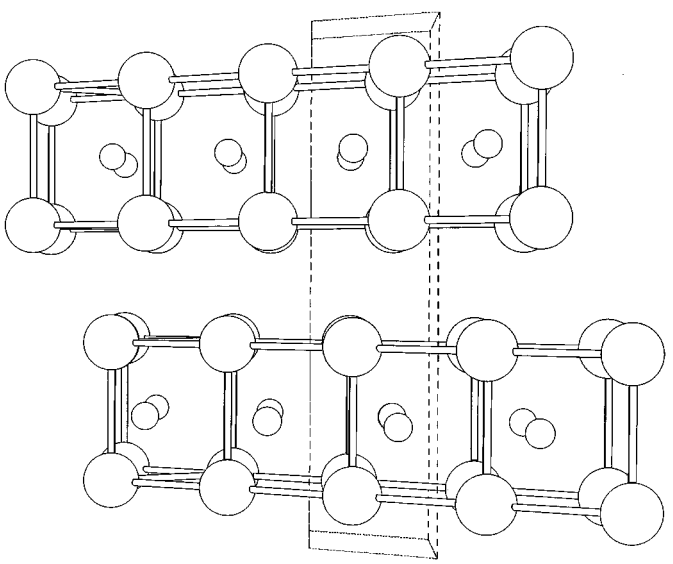

FIG. 1. Perspective view of the structure of GdI_2 along [100] of the hexagonal unit cell, large circles I atoms.

B. Sample Preparation and Characterization

GdI_2 was prepared in a solid state reaction of GdI_3 with Gd metal powder at 1100 K for three weeks in a sealed Ta tube jacketed with an evacuated silica ampoule. Due to the small separation between the melting point and the eutectic temperature, 1104 and 1098 K, respectively, special care was required to obtain the pure phase. Temperature control was carried out using a K-type thermocouple, which was in direct contact with the reaction ampoule. Good thermal insulation was used to avoid unintentional temperature change. GdI_2 is a dark metallic greenish solid that is strongly attracted to a magnet at room temperature. Since GdI_3 and especially GdI_2 are extremely moisture- and air-sensitive all handling was done under a dried argon gas atmosphere. Gd powder was obtained from Gd metal pieces (99.99%; Johnson Matthey, Karlsruhe) by hydrogenation at 873 K, grinding the brittle hydride and dehydrogenation at 1123 K. GdI_3 was prepared from Gd metal pieces and I_2 (suprapur; Merck, Darmstadt) in an evacuated, sealed fused silica ampoule. The ampoule end with the metal was heated to 1123 K for several hours while slowly increasing the temperature of the other end containing the iodine at $\approx$523 K to prevent excessive pressure build up. The product was then sublimed three times under high vacuum ($p \approx 10^{-6}$ Torr) in a tantalum crucible to yield pale yellow GdI_3.

The structure of the compound was identified by X-ray powder diffraction measurement. X-ray powder diffraction patterns taken of GdI_2 (modified Guinier technique (18), calibration with silicon, $a = 543.102$ pm, $\lambda_{CuK\alpha_1} = 154.056$ pm) showed a single phase sample with $a = 407.75(4)$ pm and $c = 1504.1(1)$ pm.

C. Magnetic and Transport Measurements

Electrical resistivity was determined on pressed pellets of 5 mm diameter and a thickness of about 1 mm by the van der Pauw method at temperature 10 K $< T <$ 380 K and in fields up to 7 T using the cryostat of a MPMS magnetometer (Quantum Design). dc currents of 10 μA or less were supplied by a Keithley 2400 sourcemeter. The voltage drop across the contacts was determined by a HP 34420A nanovoltmeter. The pellets were enclosed into a vacuum tight copper can and pressed onto four gold plated spring-contacts. The magnetic susceptibilities of powder samples

($\approx$70 mg) were measured with a MPMS SQUID magnetometer between 10 and 380 K and fields up to 7 *T*. The sample was contained in dried quartz glass ampoules under 1 bar He exchange gas to provide sufficient thermal contact. The sample containers were designed to give a negligible magnetic background signal.

III. RESULTS AND DISCUSSION

A. Electronic Structure

While GdI_2 has been studied at the extended-Hückel level by Michaelis *et al.* (12) and by Tian and Hughbanks (19) from the viewpoint of metal–metal bonding, spin-polarized calculations have not been carried out thus far. In a certain sense, GdI_2 is a magnetic analogue of $2H$-TaS_2; it is isostructural and under the reasonable assumption of a localized core of *f* electrons; it is also isoelectronic.

The spin polarized densities of states for GdI_2 are separately depicted in Fig. 2 showing the spin-up and spin-down states in the different orbital projections. The spin polarized

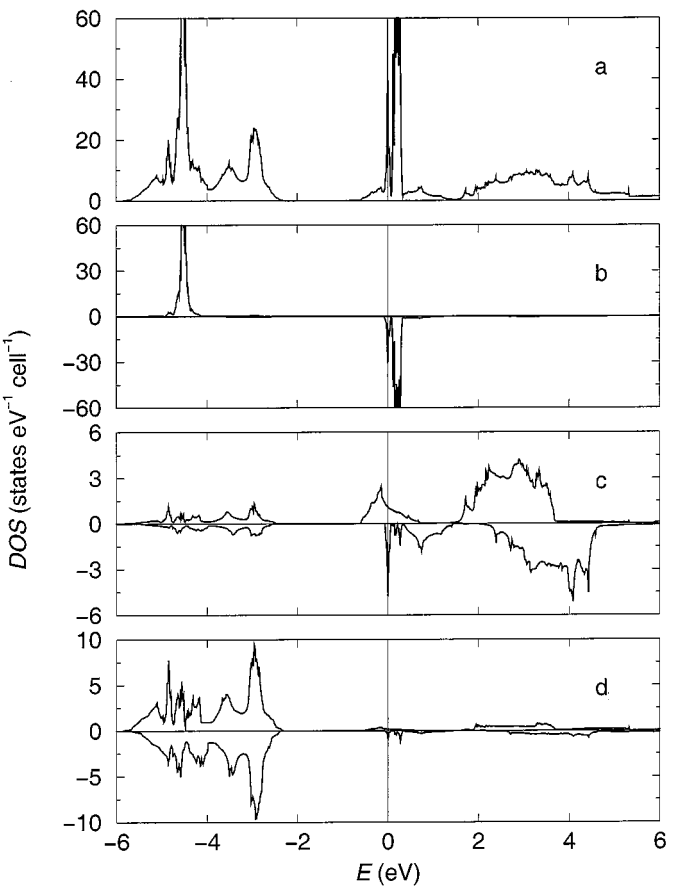

FIG. 2. LMTO densities of states for ferromagnetic GdI_2. (a) Total DOS, (b) spin-up and spin-down Gd *f*, (c) spin-up and spin-down Gd *d*, and (d) spin-up and spin-down I *p*.

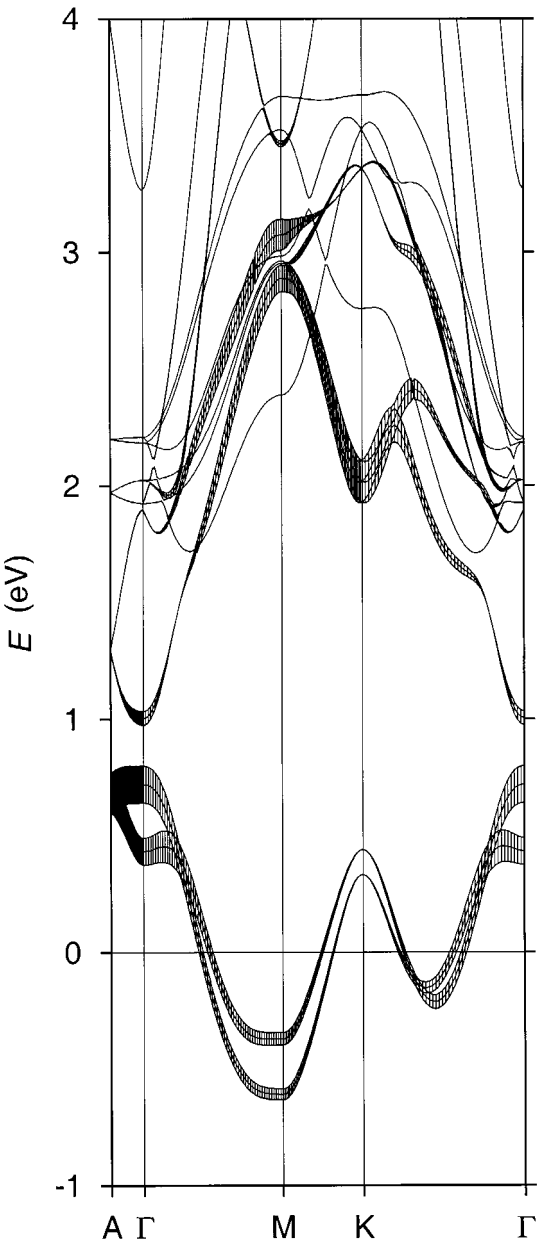

FIG. 3. Band structure of GdI_2 in fatband representation, showing the conduction band decorated with the Gd d_{z^2} contribution.

calculation on GdI_2 yields a magnetic moment of 7.36 μ_B. This is an enhancement over the value of 7 μ_B expected for the half-filled *f* band. The system is thus nearly fully spin-polarized. Examining the orbital projected DOS of GdI_2 in Fig. 3, we observe that the *f* levels are exchange split into spin-up and spin-down states with a separation of about 4.5 eV. The bulk of the *f* spin-down states is slightly (0.1 eV) above E_F. The Gd *d* bands are split due to the crystal field into lower and upper manifolds in both spin directions. It should be noted that density functional calculations, due to the neglect of certain types of electron correlations, routinely

underestimate the splitting between majority and minority *f* levels (20). As a result, the true spin-up and spin-down states are separated by a larger gap in reality, and the spin majority *f* states would be further stabilized by approximately 3–4 eV. This does not in any way affect the conclusions drawn from the calculations. The lower Gd *d* manifold crosses E_F yielding the result that GdI_2 is a magnetic metal, with the enhancement of the moment arising from polarization of the conduction band. This results in the Gd spin-up and spin-down *d* states being separated by about 1 eV. The *d* states of Gd crossing E_F have a bandwidth of a little less than 2 eV. The narrow bandwidth and the implication that electron correlation would be important in GdI_2 has been pointed out by Michaelis *et al.* (12) and Tian and Hughbanks (19). The occupied I *p* bands are stabilized by about 2.5 eV and are centered at around 4 eV below E_F. The spin polarization leaves the *p* bands of I completely unaffected.

We now point out what we believe to be an important comparison, namely that between the magnetic DOS of GdI_2 and the DOS of some ferromagnetic manganates (4, 21). The layered GMR manganate $LaSr_2Mn_2O_7$ contains Mn with an intermediate oxidation state of 3.5. Spin-polarized band structure calculations on this compound (4) which are consistent with experiment (22) show that the half-filled t_{2g} levels of the high-spin Mn atoms polarize the conduction band which is derived from the Mn e_g states. As in GdI_2, the DOS at E_F is derived from spin-up and spin-down *d* states. It is interesting that the spin-polarization of the conduction band in the manganate is provided by the t_{2g} states whereas in GdI_2, it is the half-filled Gd *f* states that polarize the Gd *d* states as E_F.

Decorating bands with an arbitrary width proportional to the sum of the weights of the corresponding orthonormal orbitals obtains "fatbands" that reveal the orbital character of bands (23). We use this tool to analyze the nature of the bands in GdI_2. The width for the decoration used here is as follows: A width that is 2.5% of the total displayed energy range corresponds to "pure" orbital character. Figure 3 shows the important d_{z^2} conduction electron spin majority fatband of GdI_2. The width of the lower branches of the two d_{z^2} bands (two because there are two formula units in the primitive unit cell) is small. In GdI_2, there is significant dispersion of d_{z^2} in the Γ–*M* direction suggesting that it interacts within the sheets of the crystal structure. d_{z^2} is clearly involved in the *M*–*M* bonding. We observe a saddle point in the band structure between Γ and *K*, 0.2 eV below E_F. Along Γ–*Z*, the dispersion of the conduction band is small suggesting quasi-2D behavior.

The Fermi surface (FS) shown in Fig. 4(a) is a cylinder around Γ. One finds regions of high dispersion (red) and of low dispersion (blue). The regions of high dispersion are found mostly along the Γ–*M* direction while the regions of low dispersion appear as pockets or knobs in the Γ–*K* direction. The tendency to nesting in the FS of GdI_2 is considerable as seen in the Fig. 4. The regions of low dispersion in the FS of GdI_2 suggest that suitable changes of the electron counts could give rise to more complete nesting.

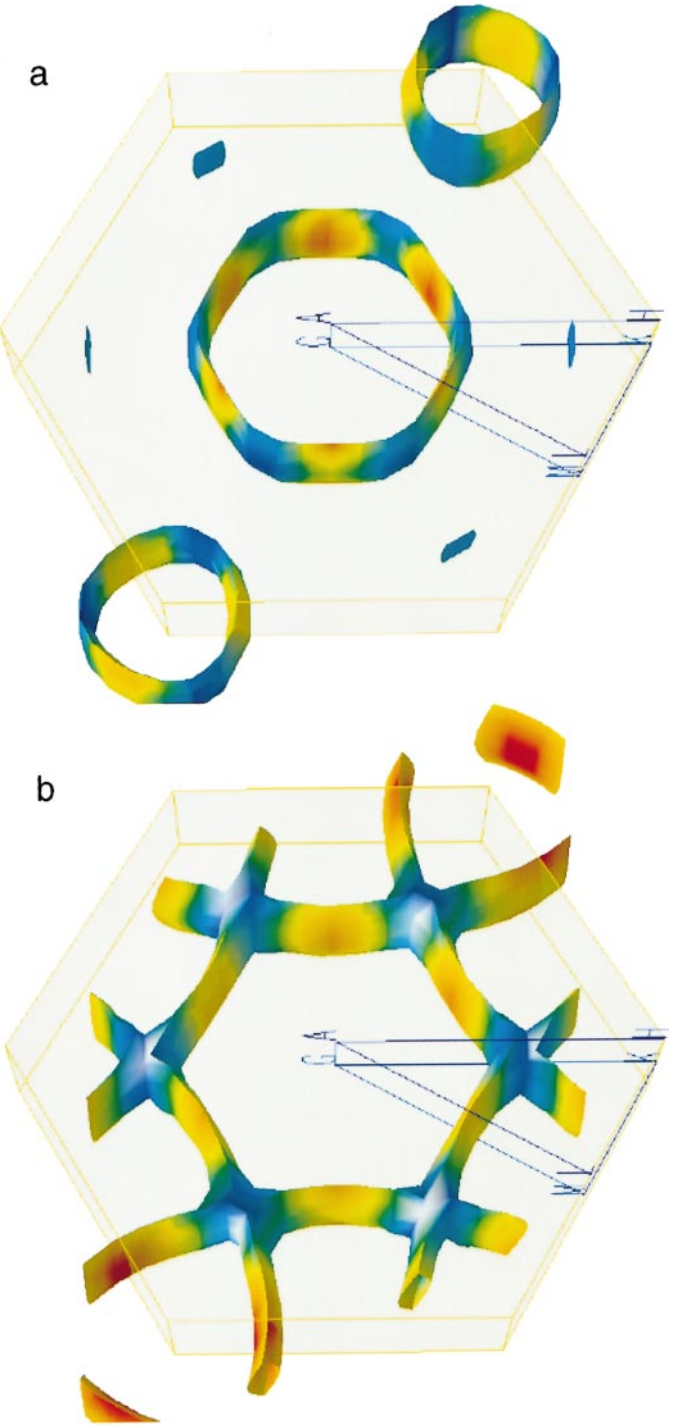

FIG. 4. (a) Fermi surface of GdI_2. (b) Energy isosurface of GdI_2 of -0.2 eV with respect to E_F. The isosurfaces are decorated with the velocities with the "hotter" electrons (toward red color) corresponding to high velocities and the "colder" (toward blue colors) corresponding to low velocities.

Considering the problem of "hole-doping" in GdI_2 through the construction of an isosurface of constant energy decorated by the velocity, we chose the absolute energy of around -0.2 eV with respect to the E_F. Within a rigid band model, this would correspond to the Fermi surface of a compound with about 0.15 holes per formula unit, equivalent, for example, to the compound $GdH_{0.15}I_2$ (12). The isosurfaces so obtained are shown in Fig. 4(b). The knobs seen in the Fermi surface are now well nested with low dispersion in the $\Gamma-K$ direction. The nesting form gives rise to a distorted X because six of them have to be fitted into the BZ (considering the whole BZ rather than a single primitive wedge). The regions of high dispersion between the X's are retained even after the hole doping. It is this combination of nested and dispersive regions in the Fermi surface (or a suitable isosurface) which led us to predict unusual magnetoresistance in GdI_2.

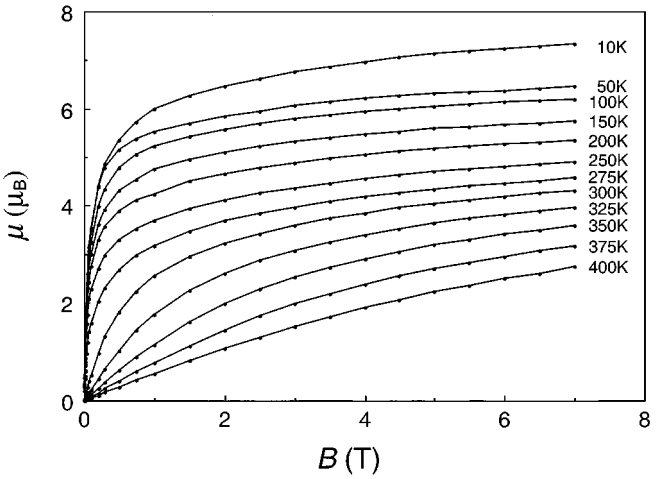

FIG. 6. Magnetization of a powder sample of GdI_2 versus magnetic field determined at constant temperatures as indicated.

B. Physical Properties

In first characterizations, GdI_2 has been described as "probably metallic" (24), and ferromagnetically ordered at 313 K (25). The electrical resistance exhibits a broad maximum around 300 K before it decreases below approximately 240 K showing an activated behavior at low temperature (12). The maximum was associated with critical fluctuations near the transition to ferromagnetism which occurred at somewhat lower temperature than in the first characterization.

The magnetic properties of our samples have initially been characterized by magnetization measurements. Figure 5 displays the temperature dependence of the magnetization measured in an external field of 10 mT. GdI_2 exhibits spontaneous magnetization below 290(5) K very close to the findings of our preceding study (12). We note that in contrast to the magnetization of our previous sample of GdI_2 (12) the present sample exhibits no shoulder above T_c. Figure 6 displays the magnetization versus field determined at various constant temperatures. At 10 K the saturation magnetization is 7.33(5) μ_B in best agreement with the value predicted by the band structure calculations. The excess of 0.33 μ_B as compared to 7 μ_B expected for seven unpaired electrons of the $4f^7$ configuration of a Gd^{3+} ion has to be attributed to the polarization of the 5*d* conduction electrons.

The electronic resistance versus temperature measured in various constant magnetic fields up to 7 T (Fig. 7) exhibits a broad anomaly centered at the Curie temperature T_c. This anomaly shifts to higher temperatures with increasing magnetic field and flattens toward the highest fields. Below

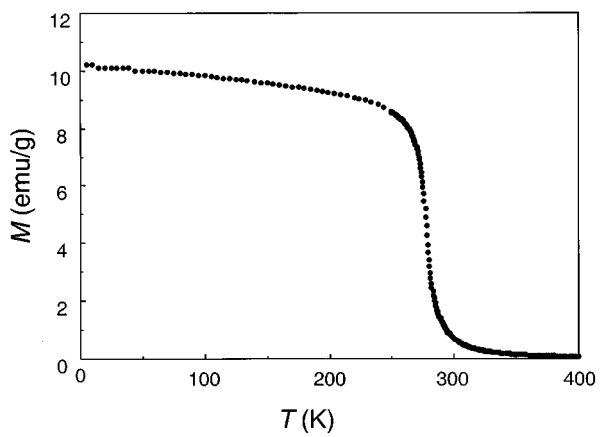

FIG. 5. Temperature dependence of the magnetization of a GdI_2 sample in a magnetic field of 10 mT.

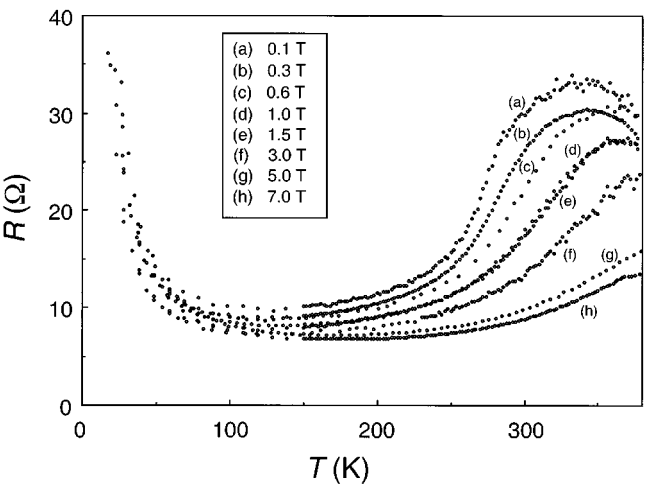

FIG. 7. Resistance of a 5 mm diameter pellet of 1 mm thickness versus temperatures as indicated.

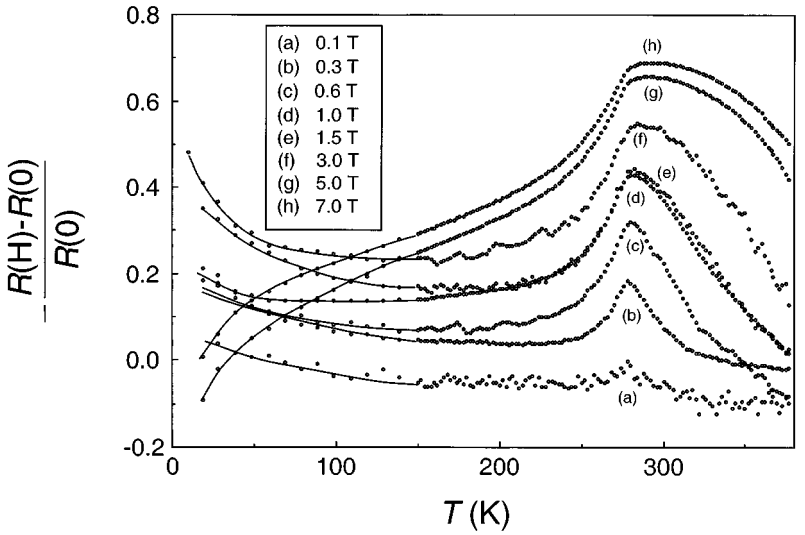

FIG. 8. Magnetoresistance $-(R(H) - R(0))/R(0)$ versus temperature for the indicated magnetic fields.

200 K the resistance shows only slight temperature- and field-dependence and increases again toward low temperatures. In view of the pronounced metal–metal bonding in reduced Gd compounds this upturn may indicate the tendency to localization through the formation of local Gd–Gd bonds (26, 27).

The magnetoresistance $-(R(H) - R(0))/R(0)$ (Fig. 8) exceeds values of 60% at room temperature and high magnetic fields. It is one and a half orders of magnitude larger than the magnetoresistance observed due to the variations of spin disorder scattering close to the ferromagnetic phase transition, e.g., in Gd (28).

In small magnetic fields the magnetoresistance to first approximation raises with a slope of $\approx 40\%/\mathrm{T}$ at room temperature. At low temperatures we observe a decrease of the magnetoresistance for the highest magnetic fields measured (5 and 7 T), the origin of which is not clear at present.

IV. CONCLUDING REMARKS

As mentioned in the Introduction, the spectacular GMR properties of the perovskite manganates are associated with the strong coupling of the charge, spin, and lattice degrees of freedom. The signature of the possibility of such coupling, we believe, is the finding of the specific patterns of instability in the Fermi surfaces. Our strategy is actually closely related to the rule of thumb that interesting electronic properties are found in materials in the vicinity of metal–insulator transitions.

Gadolinum *d* electrons with minority spin character which are present at E_F in GdI_2 are pushed into the majority channel upon the application of a magnetic field. Because of the polarization of the conduction *d* band by the underlying *f* levels, the scattering of carriers in the majority channel is significantly less than the scattering of carriers in the minority channel. This allows GdI_2 to display negative magnetoresistance, as in the perovskites (21) and the layered manganates (4). The idea that GdI_2 could display large negative magnetoresistance effects has been based on the assumptions that certain special features in the FS or suitable isosurfaces of compounds can be taken as a fingerprint for a possible superconductor, or when magnetic ions are present, which preclude superconductivity, GMR may be expected.

In this context we recollect from our discussion of the FS that we are still a little distant from optimal doping (around 0.15 holes or 0.2 eV). We speculate that hydrogen insertion in GdI_2 is one route to even more dramatic GMR effects (29). Efforts are now being directed toward the preparation of such doped compounds.

ACKNOWLEDGMENTS

We are grateful to Professor O. K. Andersen and Dr. O. Jepsen for making the LMTO program available to us. We also thank E. Brücher, G. Siegle, and S. Höhn for the susceptibility and magnetoresistance measurements.

REFERENCES

1. J. Labbé and J. Friedel, *J. Phys. (Paris)* **27,** 153 (1966).
2. J. Labbé and J. Bok, *Europhys. Lett.* **3,** 1225 (1987).
3. D. M. Newns, H. R. Krishnamurthy, P. C. Pattnaik, C. C. Tsuei, and C. C. Chi, *Physica B* **186,** 801 (1993).

4. C. Felser, R. Seshadri, A. Leist, and W. Tremel, *J. Mater. Chem.* **8,** 787 (1998).
5. C. Felser, S. Cramm, D. Johrendt, A. Mewis, O. Jepsen, G. Hohlneicher, W. Eberhardt, and O. K. Andersen, *Europhys. Lett.* **40,** 85 (1997).
6. M. N. Baibich, J. M. Broto, A. Fert, F. Nguyen Van Dau, F. Petroff, P. Etienne, G. Creuzet, A. Friedrich, and J. Chazeles, *Phys. Rev. Lett.* **61,** 2472 (1988).
7. J. Volger, *Physica* **20,** 49 (1954).
8. R. M. Kusters, J. Singleton, D. A. Keen, R. McGreevy, and R. Hayes, *Physica B* **155,** 362 (1989).
9. P. Majumdar and P. B. Littlewood, *Nature* **395,** 479 (1998).
10. J. D. Corbett, R. A. Sallach, and D. A. Lokken, *Adv. Chem. Ser.* **71,** 56 (1967).
11. H. Bärnighausen, Proceedings "Hauptversammlung der Gesellschaft Deutscher Chemiker," p. 74. München, 1997.
12. C. Michaelis, W. Bauhofer, H. Buchkremer-Hermanns, R. K. Kremer, A. Simon, and G. J. Miller, *Z. Anorg. Allg. Chem.* **618,** 98 (1992).
13. U. von Barth and L. Hedin, *J. Phys. C* **4,** 2064 (1997).
14. O. K. Andersen, *Phys. Rev. B* **12,** 3060 (1975).
15. H. L. Skriver, "The LMTO Method," Springer-Verlag, Berlin, 1984.
16. C. J. Bradley and A. P. Cracknell, "The Mathematical Theory of Symmetry in Solids." Clarendon Press, Oxford, 1972.
17. G. Krier, O. Jepsen, and O. K. Andersen, unpublished results.
18. A. Simon, *J. Appl. Cryst.* **3,** 18 (1970).
19. Y. Tian and T. Hughbanks, *Inorg. Chem.* **32,** 400 (1993); K. A. Yee and T. Hughbanks, *Inorg. Chem.* **30,** 2321 (1991).
20. V. I. Anisimov, F. Aryasetiawan, and A. L. Liechtenstein, *J. Phys.: Condens. Matter* **9,** 767 (1997).
21. W. E. Pickett and D. J. Singh, *Europhys. Lett.* **32,** 759 (1995).
22. R. Seshadri, A. Maignan, M. Hervieu, N. Nguyen, and B. Raveau, *Solid State Commun.* **101,** 453 (1997).
23. O. Jepsen and O. K. Andersen, *Z. Phys. B* **97,** 35 (1995).
24. J. E. Mee and J. D. Corbett, *Inorg. Chem.* **4,** 88 (1965).
25. A. Kasten, P. H. Müller, and M. Schienle, *Solid State Commun.* **51,** 919 (1984).
26. A. Simon, Hj. Mattausch, G. J. Miller, W. Bauhofer, and R. K. Kremer, "Handbook on the Physics and Chemistry of Rare Earths" (K. Gschneidner, Jr., Le Roy Eyring and S. Hüfner, Eds.), Vol. 15, p. 191, 1991.
27. W. Bauhofer, W. Joss, R. K. Kremer, Hj. Mattausch, and A. Simon, *J. Mag. Mag. Mater.* **104–107,** 1243 (1992).
28. T. Hiraoka and M. Suzuki, *J. Phys. Soc. Japan* **31,** 1361 (1971); K. McEwen, G. D. Webber, and L. W. Roeland, *Physica B* **86–88,** 531 (1977).
29. C. Michaelis, Hj. Mattausch, H. Borrmann, and A. Simon, *Z. Anorg. Allg. Chem.* **607,** 29 (1992); C. Michaelis, Hj. Mattausch, and A. Simon, *Z. Anorg. Allg. Chem.* **610,** 23 (1992).